European Journal of Pharmaceutics and Biopharmaceutics 142 (2019) 49–60

Contents lists available at ScienceDirect

European Journal of Pharmaceutics and Biopharmaceutics

journal homepage: www.elsevier.com/locate/ejpb

Research paper

A non-covalent antibody complex for the delivery of anti-cancer drugs

Katia Maso[a], Isabella Monia Montagner[b], Antonella Grigoletto[a], Oddone Schiavon[a], Antonio Rosato[b,c,*,1], Gianfranco Pasut[a,b,**,1]

[a] Department of Pharmaceutical and Pharmacological Sciences, University of Padova, Via F. Marzolo 5, 35131 Padova, Italy
[b] Veneto Institute of Oncology IOV-IRCCS, Padua, Italy
[c] Department of Surgery, Oncology and Gastroenterology, University of Padova, Via Gattamelata 64, 35128 Padova, Italy

ARTICLE INFO

Keywords:
Antibody-drug conjugates
Anticancer therapy
Drug delivery
PEGylation

ABSTRACT

Antibody drug conjugates (ADCs), which are obtained by coupling a potent cytotoxic agent to a monoclonal antibody (mAb), are traditionally bound in a random way to lysine or cysteine residues, with the final product's heterogeneity having an important impact on their activity, characterization, and manufacturing. A new antibody drug delivery system (ADS) based on a non-covalent linkage between a Fc-binding protein, in this case Protein A or Protein G, and a mAb was investigated in the effort to achieve greater homogeneity and to create a versatile and adaptable drug delivery system.

Recombinant staphylococcal Protein A and streptococcal Protein G were chemically PEGylated at the *N*-terminus with a 5 kDa and a 20 kDa PEG, respectively, yielding two monoconjugates with a mass of ≈50 and ≈45 kDa. Circular dichroism studies showed that both conjugates preserved secondary structures of the protein, and isothermal titration calorimetry experiments demonstrated that their affinity for mAb was approximately 10^7 M^{-1}. Upon complexation with a mAb (Trastuzumab or Rituximab), *in vitro* flow-cytometry analysis of the new ADSs showed high selectivity for the specific antigen expressing cells. In addition, the ADS complex based on Trastuzumab and Protein G, conjugated with a heterobifunctional 20 kDa PEG carrying the toxin Tubulysin A, had a marked cytotoxic effect on the cancer cell line overexpressing the HER2/neu receptor, thus supporting its application in cancer therapy.

1. Introduction

Antibody drug conjugates (ADCs), a class of anticancer therapeutics designed to selectively deliver a cytotoxic payload to tumor cells with only limited systemic toxicity towards healthy tissues, have taken important forward steps as research has successfully addressed some delivery-related obstacles linked to them. Exploiting the action of the potent cytotoxic agent conjugated to them, these therapeutics act as drug-carriers, targeting agents, and eventually as drugs themselves for a synergistic activity, selectively killing cancer cells while sparing healthy tissues [1]. Given that as single therapeutic agents, mAbs, tend to have an insufficient, although specific, clinical response, they are generally combined with other drugs. On the other hand, chemotherapeutic drugs in general are very potent but frequently do not recognize tumor cells and commonly have a relatively narrow therapeutic window, with therapeutic doses that are necessary close to the maximum tolerated ones and thus to induce severe side effects. Combining mAbs with cytotoxic drugs overcomes some of these problems because the mAb is able to selectively identify the cancer cells expressing the target antigen on the surface and consequently they can precisely delivery the drugs at the cancer cells [1].

Although developing ADCs seems simple, producing them for clinical practice is a complex process. ADCs' clinical efficacy depends on a delicate balance between multiple factors [2] including: (i) the potency

Abbreviations: ADC, antibody drug conjugate; mAb, monoclonal antibody; ADS, antibody drug system; Fc, fragment crystallisable; FcBM, Fc-binding module; PEG, polyethylene glycol; Trz, Trastuzumab; Rtx, Rituximab; TubA, Tubulysin A; DAR, drug-antibody ratio; SpA, staphylococcal Protein A; SpG, streptococcal Protein G; Fab, fragment antigen-binding; IgG, immunoglobulin G; HSA, human serum albumin; DTT, dithiothreitol; ACN, acetonitrile; TFA, trifluoroacetic acid; PDP, 3-(2-pyridyldithio)-propionate; BCA, bicinchoninic acid assay; HPLC, high performance liquid chromatography; SEC, size exclusion chromatography; RP, reverse phase; DLS, dynamic light scattering; ITC, isothermal titration calorimetry; FACS, fluorescence-activated cell sorting; FUV-CD, far UV circular dichroism

* Corresponding author at: Department of Surgery, Oncology and Gastroenterology, University of Padua, Via Gattamelata 64, I-35128 Padova, Italy.
** Corresponding author at: Department of Pharmaceutical and Pharmacological Sciences, University of Padua, Padua, Via F. Marzolo 5, I-35131 Padova, Italy.
E-mail addresses: antonio.rosato@unipd.it (A. Rosato), gianfranco.pasut@unipd.it (G. Pasut).
[1] Senior co-authorship.

https://doi.org/10.1016/j.ejpb.2019.06.012
Received 4 April 2019; Received in revised form 11 June 2019; Accepted 12 June 2019
Available online 12 June 2019

of the cytotoxic drugs [3], (ii) the expression level on the cell surface of the antigen recognized by the mAb [4], (iii) the linker used, be it hydrolysable or not, between the mAb and the drug [5], (iv) the chemical strategy at the core of the conjugation [6,7], (v) the mAb sites involved in the drug coupling process, (vi) the cellular internalization of the system and its rate [4,8], and (vii) the drug to antibody ratio (DAR) [9,10]. The drugs are usually conjugated to the lysines or cysteines of a mAb; these approaches have yielded heterogeneous ADC mixtures composed of isomers carrying a different number of drug units per antibody and a variety of positional isomers with the drug molecules linked at different positions on the antibody.

Mylotarg, Kadcyla, Adcetris, and Besponsa, the ADCs that are currently approved by the FDA, were obtained by conjugating them to surface-exposed lysines or cysteines after a partial reduction of disulfide bonds. Researchers are presently moving in the direction of developing homogenous products in the effort to obtain a better control over synthesis and characterization, improved batch-to-batch reproducibility, and better pharmacokinetic and safety profiles [11–13]. New approaches to site-specific conjugation including introducing cysteine residues by site-directed mutagenesis, utilizing enzymes to mediate the drug's coupling to specific amino acid tags in a mAb [14], inserting unnatural amino acids into the mAb backbone by genetic engineering [15,16], drug conjugation to N-Glycans in the Fc (fragment, crystallizable) moiety [17] or others are presently under investigation. As each approach means constructing a specific development strategy, it is unfortunately very difficult to benefit from knowledge already gained from other projects.

The current study presents a new approach for the delivery of anticancer drugs based on a mAbs. A given mAb non-covalently interacts with a Fc-binding molecule that carries the drug, thus forming a complex that leaves the Fab (fragment, antigen-binding) moieties free from any potentially deleterious drug conjugation/interaction effects that could reduce the antibody's affinity towards its antigen. Two bacterial proteins, Protein A (SpA) and Protein G (SpG), have been investigated as the Fc-binding molecule. SpA and SpG are cell-wall anchored receptors derived from *Staphylococcus aureus* and *Streptococci C* and *G* strains, respectively, which protect the bacteria from the host's immune system during infections [18–20] by interacting with its antibodies. These proteins are, in fact, employed in many immunochemical applications and, in particular, in antibody purification by affinity chromatography [21,22]. In terms of species reactivity, SpG binds all four subclasses of human IgG (immunoglobulins G: IgG1, IgG2, IgG3, and IgG4), but SpA is unable to recognize IgG3 [23–25]. Numerous X-ray crystallography and Nuclear Magnetic Resonance (NMR) experiments which have been reported in literature to clarify how the two proteins interact with the Fc moiety [26–33] have uncovered that the two proteins bind to nearly the same region of the Fc, the hinge region connecting the second and the third constant domains of the heavy chains (C_H2 and C_H3). Isothermal titration calorimetry experiments showed that the K_a is in the range of 10^7–10^8 M^{-1} [18]. It is the nature of the protein-protein interaction that diversifies the two complexes [26,27]. While the SpG/Fc complex is based primarily on charged and polar contacts (hydrogen and ionic bonds), the SpA/Fc complex is based on hydrophobic interactions and fewer polar contacts [34]. Both proteins contain repeating IgG-binding domains. SpA (42 kDa) consists of five highly homologous domains (named E, D, A, B, and C, in order from the N-terminus) of approximately 58-amino acids and a C-terminal X region responsible for the cell-wall attachment. Each of the five domains shows IgG-binding properties and is arranged in a three-helix bundle [35]. SpA, which has a markedly extended shape [36], contains about 50% of α-helix and 10–20% of β-strand structure [37]. As far as SpG is concerned, studies in the literature report different molecular weights and domain designations since several of the genes have been cloned and sequenced from different *streptococci* strains (the G148 strain has been the most studied one) [38–40]. The entire SpG (60 kDa) is formed by a total of about 600 amino acids, some of which arranged in three repeated domains of about 55 amino acids called C1, C2, and C3 responsible for Fc-binding [41]. Each IgG-binding domain consists of an α–helix diagonally positioned across a four stranded β-sheet [26]. The C-terminus part, which is similar to the one in SpA and forms a hydrophilic anchor that mediates the cell-wall attachment, is followed by region M, which is supposedly the transmembrane portion. SpG can also present three homologous 46-residue triple α helical domains that bind human serum albumin (HSA) [42,43].

A reduced SpG form (weighing approximately 22.8 kDa) comprising the C1, C2, and C3 domains but without any of the other regions including the HSA binding domain, was used here. An alternative IgG-binding activity of SpA and SpG is directed toward the Fab moiety. SpA is able to specifically interact with the Fab of the V_H3 family with a K_a of about 10^5–10^6 M^{-1} (Fab and Fc are non-competitive for binding) [44–47]. It was found that SpG was able to bind Fab with an affinity of 10^5 M^{-1} and without any family distinction, since the bond involves the C_H1, which is the most highly conserved region in the Fab [18,26,48].

The SpA and SpG used here acted as both Fc-binding proteins and drug carriers; the drug was not directly linked to the proteins but attached through a linker made up of a linear PEG (polyethylene glycol) chain. The use of PEG linkers of high molecular weight, 5 and 20 kDa, was preferred instead of oligoethylene glycol linkers or direct drug coupling to Fc-binding proteins in view to the known immunogenicity of SpA and SpG. The mAb/Fc-binding protein-PEG-drug system (Antibody Drug System, ADS) presents some advantages with respect to ADC approach as it provides a versatile platform upon which different mAbs can be easily interchanged depending upon the target tumor/disease to be treated. The time and cost of the investment can be reduced as the systems are generated by simply mixing the two components, the mAb and the Fc-binding protein carrying the drug. In addition, if the drug is replaced with a labelling molecule, it can be switched from a therapeutic to a diagnostic application.

Two mAbs were used here as models to study the ADS: Trastuzumab (Trz) and Rituximab (Rtx). The former is a humanized monoclonal IgG1 *k* that recognizes the extracellular domain of the HER2/neu receptor, which is over-expressed in 25–30% of breast cancers, with high affinity and specificity [49,50]. The latter is a chimeric antibody containing human IgG1 and *k* constant regions with murine variable regions that bind the human CD20 antigen, a phosphoprotein weighing 35 kDa present on normal and malignant B cells that are used to treat non-Hodgkin lymphomas [51,52].

2. Materials and methods

2.1. Materials

Recombinant Protein A and Protein G were purchased from ProSpec-Tany TechnoGene Ltd. (Israel). Trastuzumab, Rituximab, and Bevacizumab were obtained from the Veneto Institute of Oncology (IOV-IRCCS, Padova, Italy). Trastuzumab: the 150 mg product is formulated in 3.36 mg L-Histidine HCl, 2.16 mg L-Histidine, 136.2 mg α,α-trehalose, dihydrate, 0.6 mg polysorbate 20, and water for injection, USP, pH 6, at a concentration of 21 mg/ml. Rituximab: each ml of solution contains 10 mg of rituximab, polysorbate 80 (0.7 mg), sodium chloride (9 mg), sodium citrate dihydrate (7.35 mg), and water for injection, USP, pH 6.5.

Bevacizumab: the 100 mg product is formulated in 240 mg α,α-trehalose dihydrate, 23.2 mg sodium phosphate (monobasic, monohydrate), 4.8 mg sodium phosphate (dibasic, anhydrous), 1.6 mg polysorbate 20, and water for injection, USP, at a concentration of 25 mg/ml. Prior to the usage, antibodies were dialyzed against PBS pH 7.4.

Cy5-maleimide and Cy5-NHS ester were acquired from GE Healthcare (Uppsala, Sweden). N-succinimidyl-3-(2-pyridyldithio)-propionate (SPDP) was from Proteochem (Loves Park, IL, USA). BCA Protein Assay Kit for protein concentration quantification,

trifluoroacetic acid, D_2O and all other reagents including salts and solvents as well as McCoy's 5A cell medium and FACS buffer were acquired from Sigma-Aldrich s.r.l. (Milan, Italy). PEGs were from NOF Corporation (Tokyo, Japan). Precast gels for SDS-PAGE 8–16% and 4–15% were purchased from Thermo Fisher Scientific (Waltham, MA, USA) and Bio-Rad (Milan, Italy). Pierce™ Dye Removal Columns for the elimination of unconjugated Cy5 were from Thermo Fisher Scientific (Waltham, MA, USA). Tubulysin A was obtained from Tube Pharma (Wien, Austria). RPMI 1640 and DMEM cell media were from EuroClone (Milan, Italy); L-glutamine, HEPES, penicillin, streptomycin, and sodium pyruvate were obtained from Lonza (Basel, Switzerland). Heat-inactivated fetal bovine serum was from Gibco BRL (Paisley, UK). R-phycoerythrin (PE)-conjugated mouse anti-human CD20 mAb (clone 2H7) was acquired from BD Biosciences (San Diego, USA), and PE-conjugated mouse anti-human IgG1 mAb from Miltenyi Biotec (Bergisch Gladbach, Germany).

The HPLC/FPLC systems used were the following: (i) HPLC Shimadzu composed of two LC-10AD and a UV–Vis SPD-10AV detector (Kyoto, Japan); (ii) HPLC Agilent Technologies, 1260 Infinity model (Santa Clara, CA, USA); (iii) AKTA purifier (GE Healthcare, Uppsala, Sweden).

2.2. Analytical methods

NMR. NMR spectra were obtained using a Brüker Avance 400 spectrometer (Rheinstetten, Germany). operating at 400.132 MHz, and the spectra were processed with MestReNova software.

UV–Vis. Protein concentrations were determined spectrophotometrically on a Thermo Scientific Evolution 201 spectrophotometer (Waltham, MA, USA) or via BCA assay, as described elsewhere [53]. Proteins and PEGylated proteins were evaluated on the basis of their absorbance at 280 nm ($A_{280}^{0.1\%}$ SpA = 0.133, $A_{280}^{0.1\%}$ SpG = 0.90, $A_{280}^{0.1\%}$ Trastuzumab = 1.43, $A_{280}^{0.1\%}$ Rituximab = 1.63, $A_{280}^{0.1\%}$ Bevacizumab = 1.70 ml cm^{-1} mg^{-1}). Extinction coefficients at 280 nm for PEG-proteins were considered unvaried with respect to those of native proteins.

SDS-PAGE. Electrophoresis (SDS-PAGE) was performed in accordance with the Laemmli-SDS-PAGE protocol [54,55]; the gel was stained with Blue Coomassie for protein detection and with iodine for PEG detection. Electrophoretic runs were made using an Electrophoresis Power Supply 300 (Pharmacia, New Jersey, USA).

Far-UV circular dichroism (FUV-CD). FUV-CD spectra were measured on a Jasco J-810 spectropolarimeter equipped with a Peltier temperature control unit at 25 °C. The samples were dissolved in PBS pH 7.4 at a protein concentration of 0.1–0.2 mg/ml. The spectra were collected between 200 and 250 nm with an average of 3 scans and the data at each wavelength were averaged for 8 s. The sample cell path length was 1 mm. The CD data were converted to mean residue ellipticity, expressed in deg cm^2 $dmol^{-1}$ by applying the following formula:

$$\Theta_{MWR} = \Theta_{obs}(MRW)/10L[C]$$

where Θ_{obs} is the observed ellipticity in degrees, the MRW is the mean residue weight of the protein (molecular weight divided by the number of amino acids), [C] is the protein concentration in mg/ml, and L is the optical path length in centimeters.

MALDI-TOF MS. Mass spectra were obtained with a REFLEX time-of-flight instrument (4800 Plus MALDI TOF/TOF, AB Sciex, Framingham, Massachusetts, USA) equipped with a SCOUT ion source, operating in positive linear mode. A pulsed UV laser beam (nitrogen laser, λ 337 nm) generated ions that were accelerated to 25 kV. Matrix (a saturated solution of sinapic acid in water/ACN (1:1, v/v) + 0.1% TFA (v/v)) was mixed with an equal volume of sample, and 1 µl was loaded on the plate.

Dynamic light scattering (DLS). Hydrodynamic diameters were measured using a Zetasizer Nano ZS apparatus (Malvern Instruments Ltd., Worcestershire, United Kingdom) at 25 °C the results of three measurements were averaged. A series of solutions (PBS pH 7.4) with different mAb/protein molar ratios (1:0.25, 1:0.5, 1:1 and 1:2) were prepared to maintain a fixed mAb concentration and varying protein concentrations. The solutions were left to equilibrate for 1 h at room temperature and filtered with a 0.22 µm cellulose acetate centrifuge tube filter before being analyzed. The size values are reported based on volume.

Isothermal titration calorimetry (ITC). Affinity constants and binding stoichiometry between native/conjugate proteins and mAbs were determined by isothermal titration calorimetry using a VP-ITC MicroCalorimeter (GE Healthcare, Uppsala, Sweden) provided with a ThermoVac accessory for thermostatting and degassing samples. All the samples were dissolved in PBS pH 7.4. The sample cells were filled with a mAb solution that was titrated with protein solution loaded in the injector syringe. SpA and SpG concentrations ranged from 10 to 20 µM; mAbs concentration was 1–2 µM. The first injection was of 1 µl, and all the subsequent ones were of 10 µl every 240 s. The injection duration was 20 s and the stirring speed was set at 307 rpm. The experiments were conducted at 30 °C with a reference power of 9 µCal/sec. The data were analyzed using Origin 7.0, MicroCal LLC ITC and fitted to a "one set of sites" model to obtain the stoichiometry (n), the thermodynamic association constant (Ka) and enthalpy energy (ΔH°).

2.3. Synthesis of PDP-PEG-aldehyde

Heterobifunctional H_2N-PEG-COOH (5 or 20 kDa) was dissolved in acetonitrile/0.2 M sodium borate buffer pH 8 (1:2 v/v) to reach the final concentration of 100 mg/ml. A 3-fold molar excess of succinimidyl 3-(2-pyridyldithio)propionate (SPDP) was added in portions within an hour. The reaction solution was stirred at room temperature overnight. The unreacted amino groups of PEG were blocked by adding a 100-fold molar excess of acetic anhydride with respect to the mmols of PEG. The reaction was monitored by Snyder-Sobocinsky TNBS assay [56] and dialyzed against water for 48 h using a 3.5 kDa cut-off membrane. The dialyzed product was lyophilized. The degree of 3-(2-pyridyldithio)-propionate (PDP) activation was established by pyridine-2-thione assay [57] and ^1H NMR.

PDP-PEG-COOH (D_2O, δ ppm): 3.68 (m, 454.55H (for 5 kDa PEG)/1818.18H (for 20 kDa PEG), –O–[C**H**$_2$–C**H**$_2$–O]$_n$– PEG chain), 7.30 (dd, 1H, C3 pyridyl ring), 7.80 (dt, 2H, C4-C5 pyridyl ring), 8.40 (dd, 1H, C6 pyridyl ring).

The activation of the PDP-PEG-COOH carboxylic group was carried out as follows: the intermediate was solubilized in dichloromethane at a final concentration of 100 mg/ml, and a 2-fold molar excess of N,N′-dicyclohexylcarbodiimide (DCC) and hydroxybenzotriazole (HOBt) was added. After 1 h, a 3-fold molar excess of 4-aminobutyraldheyd-diethylacetal was added. If necessary, the pH was adjusted to 8 with triethylamine. The reaction was allowed to proceed under stirring at room temperature overnight. The N,N-dicyclohexylurea was removed by filtration and the solution was dropped into diethyl-ether to precipitate the product. After 1 h at − 20 °C the product was recovered by filtration and dried under vacuum. The degree of diethyl acetal derivatization was determined by ^1H NMR.

PDP-PEG-diethyl acetal (D_2O, δ ppm): 3.68 (m, 454.55H (for 5 kDa PEG)/1818.18H (for 20 kDa PEG), –O–[C**H**$_2$–C**H**$_2$–O]$_n$– PEG chain), 1.15 (t, 6H, –(OCH_2C**H**$_3$)$_2$).

The acetal was hydrolyzed at high temperature in acidic conditions to obtain the aldehyde group: a 50 mg of PEG was dissolved in 25 mM phosphate pH 2.15 at the final concentration of 50 mg/ml and maintained at 60 °C for 2 h. The solution was used directly in the next conjugation step with the protein.

2.4. N-terminal pegylation of SpA and SpG

The bacterial proteins were PEGylated with mPEG-aldehyde and with the synthesized PDP-PEG-aldehyde. Specifically, a 5 kDa MW

polymer was used for SpA and a 20 kDa PEG was employed for SpG. Proteins were site-specifically modified at the *N*-terminus by conducting the PEGylation reaction under slightly acidic conditions (pH 4.5–5.5) as described below. The protein concentration was determined by BCA assay or UV–Vis absorption at 280 nm.

The conjugated proteins were characterized by SDS-PAGE, MALDI-TOF-TOF, RP-HPLC, FUV-CD; their affinity for IgG and the stoichiometry of the complex were assessed by ITC and DLS.

2.5. Synthesis of PEG_{5kDa}-Nter-SpA and Cy5-PEG_{5kDa}-Nter-SpA

To a 2 mg/ml solution of SpA in 0.1 M sodium acetate buffer pH 5, PEG_{5kDa}-aldehyde (5-fold molar excess) was firstly added and then, after 1 h, $NaCNBH_3$ (100-fold molar excess) was added. The reaction mixture was allowed to proceed under stirring at room temperature, and its progress was monitored by RP-HPLC. After 24 h for PEG_{5kDa}-aldehyde and after 96 h for PDP-PEG_{5kDa}-aldehyde, the purification was performed by RP-HPLC with a Jupiter C18 column (250 × 4.6 mm, 300 Å, 5 μm; Phenomenex, USA) eluted with H_2O + 0.1% TFA (eluent A) and ACN + 0.1% TFA (eluent B) at 1.0 ml/min flow-rate (gradient B %: 0′ 5%, 5′ 30%, 30′ 50%, 33′ 90%, 35′ 5%). The effluent was monitored by measuring the absorbance at 226 nm for analytical and at 280 nm for purification runs. The peak corresponding to the conjugate was collected and, after the acetonitrile (ACN) was removed under vacuum, the solution was lyophilized. PEG_{5kDa}-SpA was used for *in vitro* characterization and binding studies to mAbs, and PDP-PEG_{5kDa}-SpA was conjugated to Cy5 to perform FACS (fluorescence-activated cell sorting) analysis. To a 2 mg/ml solution of PDP-PEG_{5kDa}-SpA in PBS, 1 mM dithiothreitol (DTT) was added and stirred at room temperature for 1 h in order to reduce the disulfide bond of PDP. DTT and pyridine-2-thione were removed by dialysis against degassed PBS plus 5 mM EDTA for 48 h in a nitrogen atmosphere. To a 1.2 mg/ml solution of HS-PEG_{5kDa}-SpA in PBS plus 5 mM EDTA, 2 equivalents of Cy5 maleimide (MW 817 Da) was added and stirred at room temperature overnight in the dark. The reaction was monitored by SEC-HPLC (size exclusion chromatography-HPLC) using a Zorbax GF-250 column (250 × 4.6 mm, Agilent Technologies, Palo Alto, CA) eluted with 20 mM sodium phosphate, 0.13 M NaCl pH 7 with 20% ACN (v/v) at a flow rate of 0.3 ml/min and measuring the effluent absorbance at 600 nm. The unreacted dye was removed using Pierce™ Dye Removal Columns. The solution was dialyzed against PBS and the dye coupling was quantified by UV–Vis spectrophotometer analysis following the manufacturer's instructions.

2.6. Synthesis of PEG_{20kDa}-SpG, Cy5-PEG_{20kDa}-SpG and TubA-PEG_{20kDa}-SpG

PEG_{20kDa}-aldehyde (5-fold molar excess) was added to a 2 mg/ml solution of SpG in 0.1 M sodium acetate buffer pH 4.5, and, after 1 h, of $NaCNBH_3$ (150-fold molar excess) were added. The reaction mixture was stirred at room temperature for 24 h. Analysis of PEG_{20kDa}-Nter-SpG were performed using a Jupiter C18 column (250 × 4.6 mm, 300 Å, 5 μm; Phenomenex, USA) eluting with H_2O + 0.1% TFA (eluent A) and ACN + 0.1% TFA (eluent B) at 1.0 ml/min flow-rate (gradient B %: 0′ 10%, 25′ 60%, 28′ 90%, 30′ 10% B). The effluent was monitored at 226 nm. The purification was carried out with DEAE-Toyopearl 650 M column (1.6 × 4.5 cm) working at a flow-rate of 1.0 ml/min and registering the absorbance at 280 nm (buffer A: 10 mM Tris-HCl pH 8 and buffer B: 10 mM Tris-HCl, 0.1 M NaCl pH 8; gradient B%: 0′ 0%, 10′ 0%, 80′ 100%, 105′ 100%, 110′ 0%). The peak of the conjugated protein was collected and concentrated with Amicon Ultra Centrifugal filters. The product was dialyzed against PBS. As in the case of SpA, PEG_{20kDa}-SpG was used for *in vitro* characterization and antibody binding studies to mAbs; PDP-PEG_{20kDa}-SpG was conjugated to Cy5 to perform FACS analysis. To a 1.2 mg/ml solution of PDP-PEG-SpG in DEAE eluting buffers, 100 equivalents of DTT was added and stirred for 1 h at room temperature in order to obtain HS-PEG-SpG. DTT and pyridine-2-thione were removed by SEC chromatography using a Superdex® 200 Increase 10/300 GL column (30 cm × 10 mm, 8.6 μm particle size, GE Healthcare) eluting with PBS and 5 mM EDTA pH 7.4 at 0.5 ml/min and measuring absorbance at 280 nm. To the purified peak of HS-PEG-SpG, 3 equivalent of Cy5-maleimide was added. The reactions were allowed to proceed in the dark overnight at room temperature. Unreacted dye was removed using Pierce™ Dye Removal Columns and dye removal was confirmed by SEC-HPLC. The solution was dialyzed against PBS, and dye coupling was quantified by UV–Vis spectrophotometer analysis following the manufacturer's instructions.

Methanol was added to HS-PEG_{20kDa}-SpG peak eluted by Superdex® 200 Increase 10/300 GL column for the synthesis of TubA-PEG_{20kDa}-SpG in order to achieve a final concentration of 30% v/v that was necessary to guarantee Tubulysin A (TubA) solubility. Three equivalents of toxin (MW 1012.49 Da) were added to the protein solution and the reaction was stirred overnight at room temperature. The reaction mixture was then dialyzed against PBS and the insoluble TubA was removed by filtering the solution through a 0.22 μm filter. The reaction was monitored using a Jupiter C18 column (250 × 4.6 mm, 300 Å, 5 μm; Phenomenex, USA) working at a flow-rate of 1.0 ml/min and registering the absorbance at 254 nm (eluent A: 10 mM ammonium bicarbonate pH 7 and eluent B: ACN; gradient B%: 0′ 40%, 10′ 52%, 15′ 70%, 18′ 90%, 25′ 40%). The sample was concentrated using Amicon®. The sample was treated with 10 mM DTT for drug loading quantification, in order to liberate the toxic substances, and injected into a Jupiter C18 column (250 × 4.6 mm, 300 Å, 5 μm; Phenomenex, USA) working at a flow-rate of 1.0 ml/min and registering the absorbance at 254 nm (eluent A: 10 mM ammonium bicarbonate pH 7 and eluent B: ACN; gradient B%: 0′ 40%, 10′ 52%, 15′ 70%, 18′ 90%, 25′ 40%). TubA loading was quantified using a calibration curve of standard toxin solutions.

2.7. Preparing Cy5-mAbs

A 5–10 fold molar excess of Cy5-NHS (MW 791.99 Da) was added to a 1–2 mg/ml solution of a mAb (Trz, Rtx and Bevacizumab) in PBS, and the mixture was stirred in the dark overnight at room temperature. After the unreacted dye was removed with Pierce™ Dye Removal Columns, mAbs concentration and dye loading were calculated by UV–Vis spectroscopy following the manufacturer's instructions.

2.8. Tumor cell lines

The following human tumor cell lines were used: BL-41, a Burkitt lymphoma B cell line; Raji, a lymphoblast-like cell line derived from a Burkitt lymphoma; LCL, a lymphoblastoid cell line generated by Epstein-Barr virus (EBV) infection of peripheral blood mononuclear cell (PBMC); Jurkat, a T cell lymphoma cell line; IGROV-1 and SKOV-3, which are ovarian adenocarcinoma cell lines; MDA-MB-231 and SK-BR-3, which are breast cancer cell lines.

The cells were grown in RPMI 1640 (except for MDA-MB-231 and SK-BR-3, which were cultured in McCoy's 5A and DMEM, respectively) supplemented with 10% (v/v) heat-inactivated fetal bovine serum, 2 mM L-glutamine, 10 mM HEPES, 200 U/ml penicillin, 200 U/ml streptomycin and 1 mM sodium pyruvate, hereafter referred as to complete medium.

The cell lines were maintained at 37 °C in a humidified atmosphere containing 5% CO_2.

2.9. Cytometry analysis

CD20 expression in BL-4, Raji, LCL, and Jurkat cell lines, and HER2/neu expression in IGROV-1, SKOV-3, MDA/MB-231, and SK-BR-3 were evaluated by flow cytometry. The cells (3×10^5/sample) were re-suspended in 50 μl fluorescence-activated cell sorter (FACS) buffer

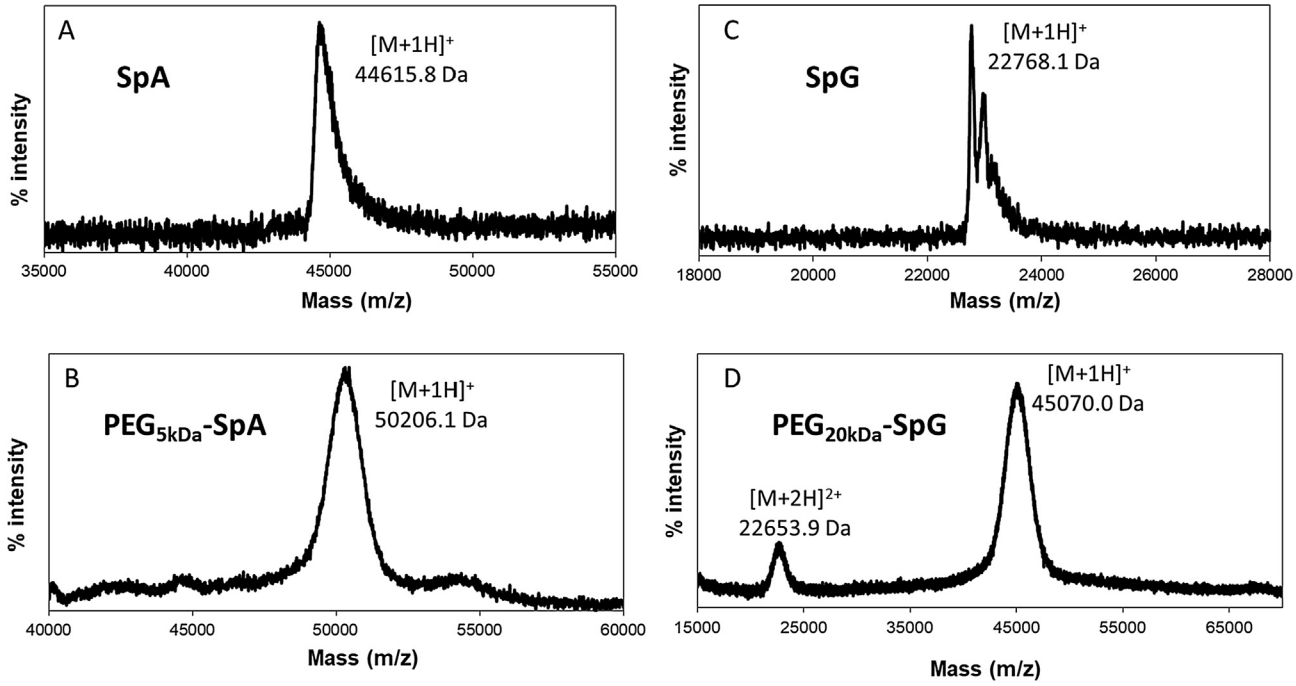

Fig. 1. MALDI-TOF mass spectroscopy analysis of (A) SpA (44615.8 Da), (B) PEG_{5kDa}-SpA (50206.1 Da), (C) SpG (22768.1 Da) and (D) PEG_{20kDa}-SpG (45070.0 Da).

(0.9% NaCl solution containing 2% bovine serum albumin and 0.02% NaN3), and stained at 4 °C for 30 min with PE-conjugated mouse anti-human CD20 mAb or with Trz (1:100), and then for another 30 min at 4 °C with PE-conjugated mouse anti-human IgG1 mAb. Before they were analyzed, the cells were washed twice, resuspended in FACS buffer, and analyzed with a flow cytometer FACS-CALIBUR (Becton Dickinson, Erembodegem, Belgium). Data analysis was performed using the FlowJo 7.6.5 data analysis software package (TreeStar, USA).

The capacity of an ADS Cy5-PEG-Protein/mAb to bind the target antigen expressed on the cell surface was then assessed by other experiments. mAbs were added to Cy5-PEG_{5kDa}-SpA or Cy5-PEG_{20kDa}-SpG PBS solutions at the binding stoichiometry determined by ITC analysis as follows: a 1.6-fold molar excess of Rtx and 1-molar excess of Trz were added to Cy5-PEG_{5kDa}-SpA and Cy5-PEG_{20kDa}-SpG, respectively. The solutions were diluted with PBS in order to achieve a mAb final concentration of 0.2 mg/ml. Cy5-PEG_{5kDa}-SpA/Rtx ADS was tested on $CD20^+$ and $CD20^-$ cell lines, while Cy5-PEG_{20kDa}-SpG/Trz ADS on $HER2/neu^+$ and $HER2/neu^-$ cell lines. Cy5-PEG_{20kDa}-SpG and Cy5-PEG_{5kDa}-SpA in an ADS form with an unspecific IgG were used as a negative control; Trz-Cy5 and Rtx-Cy5 were used as positive controls. The samples were tested at the same Cy5 and mAb concentrations between Cy5-PEG-protein/mAb ADSs and their positive and negative controls.

Competition experiments were also performed to verify if the Cy5-PEG-protein/mAb ADS complexes were stable after incubation with a competitive mAb that did not recognize the target cells, or if the non-specific mAb displaced the mAb of the starting complex. An equivalent amount of nonspecific mAb, with respect to the starting mAb in the ADS, was added to a Cy5-PEG-protein/mAb ADS solution incubated for 30′ and tested by FACS analysis.

2.10. Cytotoxicity assay

The *in vitro* cytotoxicity of TubA-PEG_{20kDa}-SpG/Trz, and as controls Trz and TubA-PEG_{20kDa}-SpG and TubA-PEG_{20kDa}-SpG/Rtx, were assessed in MDA-MB-231 and SK-BR-3 cell lines using the ATPlite luminescence adenosine triphosphate (ATP) detection assay system (PerkinElmer, Zaventem, Belgium), according to the manufacturer's instructions.

Briefly, the cells were resuspended in complete medium and seeded into 96-well flat-bottomed plates (8×10^3/well). The following day, different drug concentrations were added (final volume, 100 µl/well) for 72 h. At day 4, 50 µl of lysis solution was added to each well; then 50 µl of substrate solution was added and the TopCount Microplate Counter (PerkinElmer) was used for the final luminescence counting. Within each experiment, determinations were performed in duplicate; the experiments were repeated two times for each cell line. The percentage of cell survival was calculated by determining the counts per second (cps) values using the formula: $[(cps_{tested} - cps_{blank})/(cps_{untreated\ control} - cps_{blank})] \times 100$, with cps_{blank} referring to the cps of wells that contained only medium and ATPlite solution. IC_{50} values were calculated from semi-logarithmic dose-response curves by linear interpolation.

3. Results and discussion

3.1. Pegylation of SpA and SpG

SpA and SpG have been successfully exploited as tools for the proper orientation of antibodies in a variety of immunoassays, such as ELISA [58], magnetic beads [59] and biosensors [60,61]. It has been shown that antibodies immobilization through SpA and SpG leads to a uniform orientation of Fab regions that remain well accessible for the interaction with the antigen. These immunoassays illustrate how antibodies preserve their antigen-binding capacity even when they are in complexes with SpA and SpG. Exploiting this concept, we aimed to develop an antibody-drug system in which the drug cargo is non covalently and selectively connected to the Fc region of the targeting mAbs thanks to the presence of these bacterial proteins.

The two Fc-binding molecules were site-specific PEGylated at the *N*-terminus by performing the reaction at slightly acidic conditions in order to exploit the different pK_a values between the *N*-terminal α-amino and the ε–amino groups of lysines, the latter being protonated and consequently less reactive in acid buffers [62,63]. The rationale for the use of PEG was two-fold, firstly for reducing the known immunogenicity of SpA and SpG, and secondly, because SpG tends to

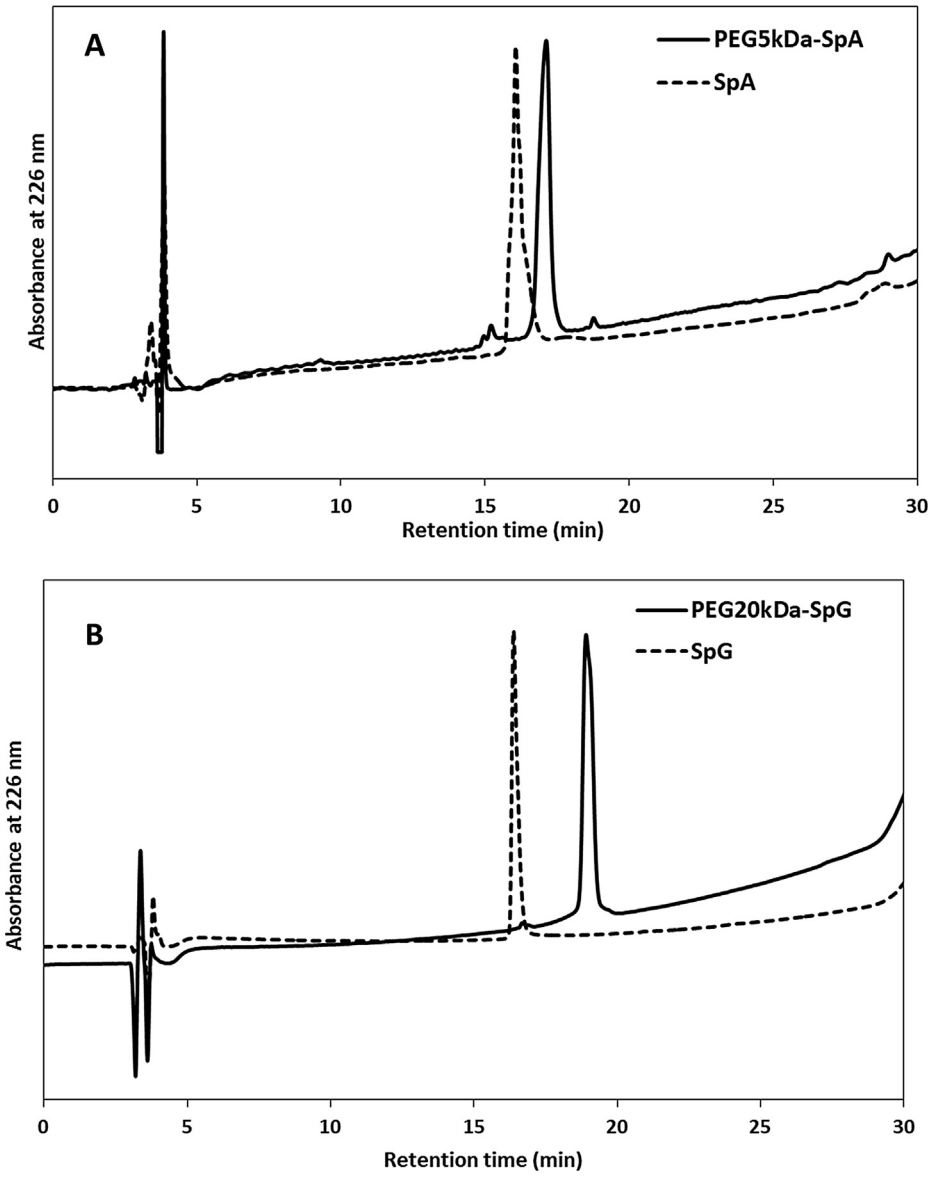

Fig. 2. (A) RP-HPLC chromatograms of SpA (dotted line) and PEG_{5kDa}-SpA and (B) RP-HPLC chromatograms of SpG (dotted line) and PEG_{20kDa}-SpG (continuous line). Samples were injected in a Phenomenex Jupiter C18 column (250 × 4.6 mm, 300 Å, 5 µm), eluting at 1 ml/min with H_2O MilliQ + 0.1% v/v TFA (eluent A) and ACN + 0.1% v/v TFA (eluent B) and reading the absorbance at 226 nm. Gradient B% for (A): 0 min 10%, 25 min 60%, 28 min 90%, 30 min 10%. Gradient B% for (B): 0 min 5%, 5 min 30%, 30 min 50%, 33 min 90%, 35 min 5.

forms insoluble complexes with the proposed mAbs. In fact, we found that upon addition of SpG to the mAb solutions, a visible precipitate was immediately formed (as reported also elsewhere [23]). The same behavior was preserved after *N*-terminal PEGylation of SpG with a PEG 5 kDa, consequently for SpG a PEG 20 kDa was used. Of note, also multiPEGylation of SpG with PEGs of 2 and 3 kDa at Lys residues yielded conjugates (with an average of 2 PEG chains per protein) that did not form insoluble complexes with mAbs but, at the same time, were still able to bind the Fc of a IgG. However, we decided to investigate further only the *N*-terminal conjugate owing its superior homogeneity and batch-to-batch reproducibility.

PEGylation reactions of SpA and SpG were performed both with PEG-aldehyde, to study the reaction conditions, and with 3-(2-pyridyldithio)-propionyl-PEG-aldehyde (PDP-PEG-aldehyde) to produce a conjugate with a suitable reactive group for drug conjugation, via thiol conjugation. PEGylated SpA conjugates were purified by RP-HPLC (Fig. S1, A), and the SpG ones by anion exchange chromatography (Fig. S1, B). The purified monoconjugates were characterized by RP-HPLC, SDS-PAGE, MALDI-TOF and FUV-CD.

The PEG_{5kDa}-SpA appeared as a single smeared band in SDS-PAGE at 55 kDa (Fig. S2, A, lanes 2 and 2′) and PEG_{20kDa}-SpG as a single smeared band at about 70 kDa (Fig. S2, B, lanes 3 and 3′). PEG had a large hydrodynamic volume that conferred an elevated apparent molecular weight (MW) to PEGylated proteins in SDS-PAGE that did not correspond to the MW determined by mass spectrometry. In fact, MALDI-TOF analysis revealed a MW of 50206.1 Da for PEG_{5kDa}-SpA and 45070.0 Da for PEG_{20kDa}-SpG (Fig. 1: B and D, respectively). PEG's polydispersity was also mirrored in the typical smeared bands of the conjugates. It is noteworthy that the migration of SpG in the electrophoretic gel was affected by the protein's elongated fibrous shape, resulting in a higher apparent MW of 37 kDa (Fig. S2, B, lane 1). Indeed, this anomalous behaviour was already pointed out by Goward [64] and other authors [23,41,65] that observed an apparent MW of 35 kDa by SDS-PAGE, in conflict with the predicted MW of about 20 kDa. Among the possible explanations, they reported an excessively elongated structure of the molecule in SDS or low SDS binding to the protein.

Both SDS-PAGE and MALDI-TOF analysis confirmed that the conjugates were monoconjugates, and that the purification process from the native proteins and the diPEGylated species was successful. The RP-HPLC profiles (Fig. 2) show that the peaks of the proteins shifted to higher retention times after PEGylation due to the polymer's presence.

Both SpA and SpG have predominantly α-helix structures in physiological conditions, clearly shown by the FUV-CD spectra (Fig. 3). CD experiments were performed in the effort to verify if PEGylation

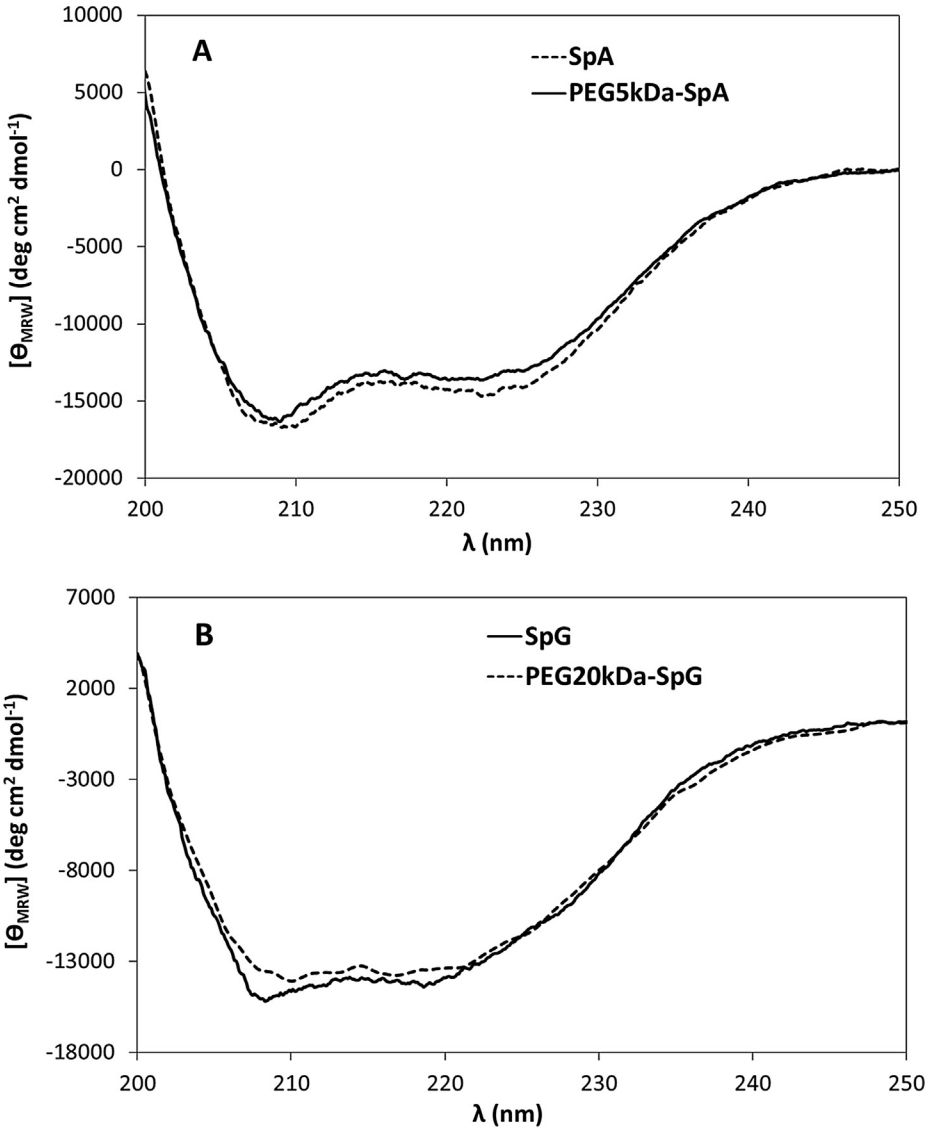

Fig. 3. FUV-CD spectra of (A) SpA (dotted line) as opposed to PEG_{5kDa}-SpA (continuous line), (B) SpG (dotted line) and PEG_{20kDa}-SpG (continuous line).

Table 1
The thermodynamic parameters of binding native and PEGylated SpA and SpG against Rtx and Trz, respectively, at 30 °C in PBS pH 7.4. Trz = Trastuzumab, Rtx = Rituximab, N = protein/mAb ratio, nd = not determinable.

Complex	K_a (M^{-1})	ΔH° (kJ/mol)	ΔS° [kJ/(K mol)]	N
SpA/Rtx	$(2.6 \pm 1.7) \times 10^8$	−438.1 ± 16.7	−1.3	0.41 ± 0.01
PEG_{5kDa}-SpA/Rtx	$(4.7 \pm 1.2) \times 10^7$	−407.5 ± 11.1	−1.2	0.62 ± 0.11
SpG/Trz	nd	nd	nd	nd
PEG_{20kDa}-SpG/Trz	$(6.1 \pm 1.0) \times 10^7$	−196.8 ± 2.8	−0.5	1.05 ± 0.01

modified the secondary structure of the protein thus potentially altering its binding properties. The profiles of the FUV-CD of conjugates were superimposable with those of the native forms.

PDP-PEG conjugates of SpA and SpG were obtained following the methods optimized with mPEG-aldehyde and characterized as shown above. The conjugates were then treated with DTT to reduce the PDP group and to obtain the free thiol one (the size exclusion chromatography of HS-PEG_{20kDa}-SpG is shown in Fig. S3) for Cy5 maleimide or TubA conjugation (TubA structure, RP-HPLC and mass spectrometry characterizations are shown in Fig. S4). Characterization of the conjugates is shown in Figs. S2, S5–S7. TubA/SpG molar ratio was 0.9 as determined after TubA release by DTT treatment and TubA quantification by RP-HPLC (Fig. S8). A TubA derivative with a 3-pyridyldithio propionate reactive group was used here to tether the toxin to the PEG end via a disulfide bond.

3.2. Binding studies of PEGylated SpA and SpG to mAbs

Isothermal titration calorimetry (ITC). ITC was used to determine K_a and the binding stoichiometry between mAbs and PEGylated proteins. All the titrations were carried out in PBS, which has a relatively small and negligible heat of ionization. The binding properties of SpA and its PEGylated form were evaluated against Rtx. As far as SpG was concerned, only the PEGylated form of the protein against Trz was analyzed because the native SpG yielded a precipitate immediately after it was mixed with the mAb. The aggregate is probably a consequence of SpG interactions also with the Fab beside the Fc regions. The thermodynamic parameters of the complexes' formation are shown in Table 1.

Despite having five IgG-binding domains, unmodified SpA was able to bind an average of 2.4 molecules of Rtx with an affinity of 2.6×10^8 M^{-1} (Fig. 4). PEG_{5kDa}-SpA showed instead an approximately 5-fold

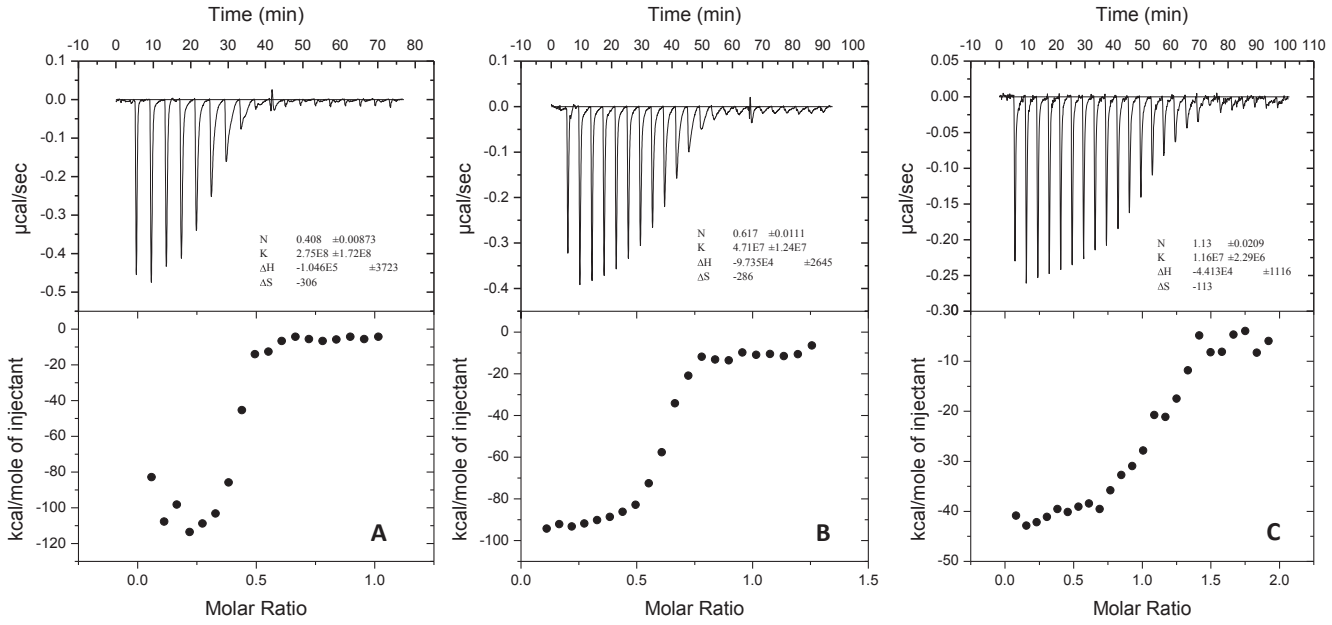

Fig. 4. Thermograms (top) and binding isotherms (bottom) of the titration study of (A) SpA/Rtx, (B) PEG_{5kDa}-SpA/Rtx and C) PEG_{20kDa}-SpG/Trz in PBS pH 7.4 at 30 °C.

Table 2
DLS analyses of the complexes between mAbs and PEGylated proteins at different mAb/protein molar ratios.

Species	mAb/protein molar ratio	Diameter (nm)	PdI
Rtx	–	11.1 ± 0.9	0.28
Trz	–	11.0 ± 0.9	0.20
SpA	–	9.4 ± 0.8	0.31
PEG_{5kDa}-SpA	–	12.3 ± 0.9	0.27
SpG	–	3.5 ± 0.09	0.35
PEG_{20kDa}-SpG	–	16.5 ± 0.7	0.56
Complex			
PEG_{5kDa}-SpA/Rtx	1:0.25	16.6 ± 0.2	0.15
	1:0.5	23.6 ± 0.5	0.14
	1:1	17.5 ± 0.7	0.20
	1:2	14.2 ± 0.3	0.14
PEG_{20kDa}-SpG/Trz	1:0.25	12.5 ± 0.8	0.38
	1:0.5	31.5 ± 0.5	0.19
	1:1	55.8 ± 0.9	0.09
	1:2	28.0 ± 0.6	0.20

decrease in affinity and a stoichiometry of 1.6. In most cases, PEGylation causes a decrease in the biological potency of proteins because of a reduction in binding affinity owing to partial steric entanglement [66] but also by reducing the mobility of the conjugated protein that has a bigger hydrodynamic volume.

PEGylated SpG showed a molar ratio of one molecule of PEG_{20kDa}-SpG per Trz and a K_a of 6.1×10^7 M^{-1}. Interestingly, PEGylation did not have a strong effect on the binding affinity of SpA and SpG even when a PEG 20 kDa was conjugated. As reference for SpG we took into account the affinity reported by Lund and coworkers and obtained by ITC using experimental conditions very similar to ours [18]. Previous determination of SpA and SpG affinity for mAbs were done with techniques different from ITC, making the comparison between our results and literature data more difficult. Of note, the recombinant form of SpG used by Lund was not forming insoluble complexes and the K_a could be measured resulting in the range of 10^8 M^{-1}.

Dynamic light scattering (DLS). Average SpA and SpG diameters were, respectively, 9.4 and 3.5 nm, and they rose to 12.3 and 16.5 nm for PEG_{5kDa}-SpA and PEG_{20kDa}-SpG, respectively (Table 2). Rtx and Trz diameters were approximately 11 nm. The technique was used to determine the average diameter of the complexes in solutions at increasing protein/mAb ratios (Table 2). The maximum complex sizes were reached at the protein/mAb ratio that was similar to the binding stoichiometry determined by ITC analysis (i.e., approximately 2 for SpA/Rtx and approximately 1 for SpG/Trz). For all the other ratios, the sizes were reduced because the instrument showed a size that was the average of the complex size and the size of the compound in excess, namely the Fc-binding protein or the mAb. This investigation confirmed the binding stoichiometry found by ITC.

3.3. CD20 and HER2/neu receptor expression on target cancer cell lines

Flow cytometry analysis was carried out to assess CD20 and HER2/neu expression on a panel of human tumor cell lines. The results showed that CD20 was intensely expressed on all the B cell lines examined except on the Jurkat one (Fig. S9, A). High HER2/neu expression was found instead in SKOV-3 and SK-BR-3, but the receptor was absent in the IGROV-1 and MDA-MB-231 cells (Fig. S9, B).

3.4. An analysis of the interaction between the ADS and cancer cell lines

The polymer moiety was labeled with the Cy5 fluorophore in order to assess the capacity of a PEG-protein/mAb ADS to bind the target antigen expressed on the cell surface. Cy5-PEG_{5kDa}-SpA/Rtx was tested on Jurkat CD20 negative cell line and BL-41, LCL and Raji CD20 positive cells, while Cy5-PEG_{20kDa}-SpG/Trz on HER2/neu$^-$ (IGROV-1 and MDA-MB-231) and HER2/neu$^+$ (SKOV-3 and SK-BR-3) cells. The results showed that the Cy5-PEG_{5kDa}-SpA/Rtx ADS was bound to the CD20$^+$ targeted cancer cells as well as the free Rtx. Indeed, the geometric mean of the positive cells was significantly higher with respect to that of the ADS prepared with the non-specific mAb (Bevacizumab) (Fig. 5, A). The Cy5-PEG_{20kDa}-SpG/Trz was also bound to the HER2/neu$^+$ cancer cell line, and the geometric mean was similar to that of the respective free Trz (Fig. 5, B). Neither of the three negative cell lines interacts with the mAbs and the ADSs.

Competition experiments were also performed to assess the stability of a preformed Cy5-PEG-protein/mAb ADS complex after incubation with a competitive mAb that did not recognize the tumor cell line; this was done to verify if the mAb in the starting ADS could be displaced by another one. The incubation used a non-specific mAb, Bevacizumab,

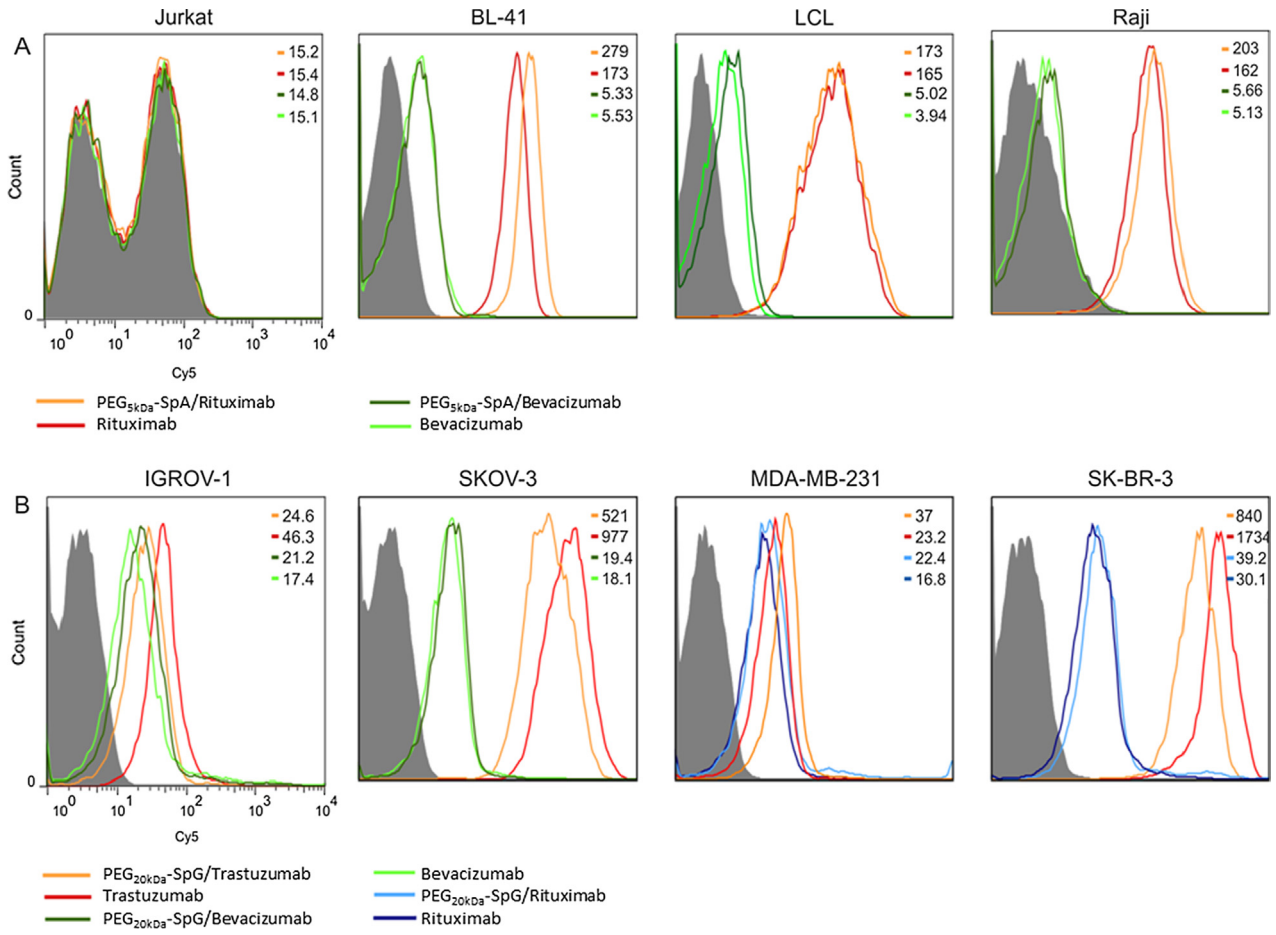

Fig. 5. ADS binding evaluation in different tumor cell lines. Interaction experiments in (A) B-cells and (B) ovarian adenocarcinoma and breast cancer cell lines. The grey shaded areas depict autofluorescence control. The values in the upper-right corner of each panel represent the geometric mean. Data are representative of three independent experiments.

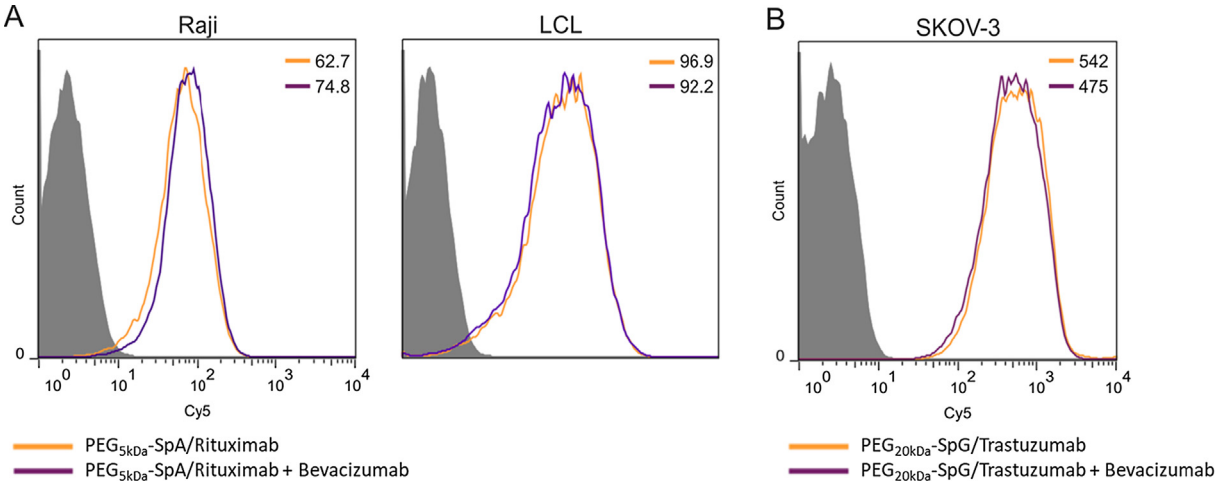

Fig. 6. ADS competition experiments in target tumor cell lines. The stability of ADS complex was evaluated in B-cells and ovarian adenocarcinoma cell line, (A) and (B), respectively. The grey shaded areas depict autofluorescence control. The respective geometric mean values are indicated at the upper-right corner of each panel. Data are representative of three independent experiments.

which is unable to recognize the cancer cell lines here tested. Cytofluorimetric analysis disclosed that the non-specific mAb did not perturb the strong, specific binding of the preformed ADSs of Rtx or Trz (Fig. 6, A and B). Indeed, the geometric mean values were comparable when B-cells were incubated with Cy5-PEG$_{5kDa}$-SpA/Rtx or with Cy5-PEG$_{5kDa}$-SpA/Rtx mixed with Bevacizumab (Raji 62.7 and 74.8; LCL 96.9 and 92.2, respectively); similar results were obtained for the cells incubated with Cy5-PEG$_{20kDa}$-SpG/Trz or with the Cy5-PEG$_{20kDa}$-SpG/Trz and Bevacizumab mixture (524 and 475, respectively). Although these experiments cannot replicate the real *in vivo* context, where the host antibodies can displace the selected mAb in an ADS construct, the results here presented are encouraging because they did not show any

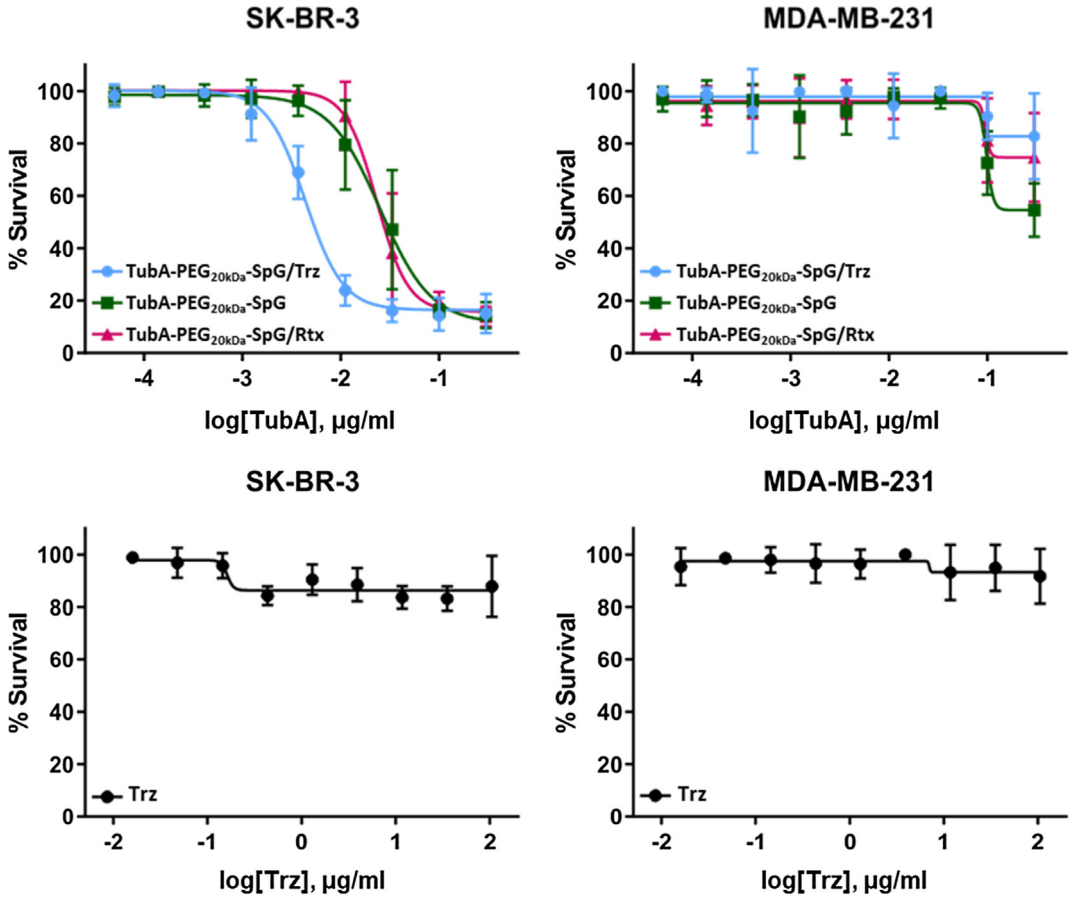

Fig. 7. Survival curves of human breast cancer cell lines in response to ADSs, TubA-PEG_{20kDa}-SpG/Trz and TubA-PEG_{20kDa}-SpG/Rtx and to non-targeted TubA-PEG_{20kDa}-SpG. The growth inhibition effect was evaluated by ATPlite assay. The table shows the mean ± SD of two independent experiments. For each experiment, the IC_{50} was calculated from each single semi-logarithmic dose-response curve by linear interpolation, and the values that were obtained, reported in µg/ml in free drug equivalents, were averaged.

perturbation of the ability of the specific prepared ADS to recognize the target cells after challenging with an unspecific antibody.

3.5. *In vitro inhibition of tumor growth by ADS*

For further developments we selected SpG as Fc-binding molecule because its PEGylated form showed a 1:1 binding ratio with mAbs, thus allowing a reduction of heterogeneity and better reproducibility. The *in vitro* cytotoxicity of ADS was investigated using TubA-PEG_{20kDa}-SpG/Trz against the targeted cancer line. TubA was chosen as the active cargo because of its potent cytotoxicity. Antimicrotubular agents, in fact, which block cell growth by inhibiting mitosis, are considered some of the most appropriate payloads for ADC development given their high activity levels (within the sub-nanomolar range). TubA was tethered by means of a disulfide bond to one PEG end. Disulfide bridges have, in fact, been largely exploited in drug delivery systems to promote the drug's release after cellular internalization [67]. Drug release is triggered by the reducing environment of the cytoplasm; the concentrations of reduced glutathione are 100–1000 times higher than those in the plasma [68].

The cells were incubated during the experiment with escalating doses of ADS, TubA-PEG_{20kDa}-SpG, or Trz alone. The HER2-specific ADS (TubA-PEG_{20kDa}-SpG/Trz) exhibited high cytotoxic potency in the HER2-expressing SK-BR-3 cancer cells, with IC_{50} values of 0.006 µg/ml ± 0.001 (drug equiv.) (Fig. 7). The same ADS was more than 16-fold less potent in the HER2/neu negative MDA-MB-231 human breast cancer cells with IC_{50} values of 0.101 µg/ml ± 0.015, thus confirming that Trz in the ADS plays an active role in binding HER2/neu receptor and yields an improved cytotoxic effect. TubA, instead, exhibited a similar cytotoxic efficacy in both cell lines (SK-BR-3, IC_{50} = 0.045 µg/ml ± 0.001; MDA-MB-231, IC_{50} = 0.085 µg/ml ± 0.012), while Trz had no cytotoxic effect in any culture. In addition, the IC_{50} values of the non-targeted counterpart (TubA-PEG_{20kDa}-SpG) and the non-HER2-specific ADS (TubA-PEG_{20kDa}-SpG/Rtx) in the SK-BR-3 and MDA-MB-231 cancer cells were very similar, which again supports the relevance of Trz for selective cytotoxicity of its ADS construct in cancer cells HER/neu^+. The reduced cytotoxic sensitivity of MDA-MB-231 to the ADS is due to the lack of HER2/neu expression in this cell line on the one hand and on the other, it further supports the HER2/neu mediated binding and internalization of the ADS in the SK-BR-3 cell line (HER2/neu^+).

This *in vitro* cytotoxicity investigation clearly showed that the non-covalently bound Trz in the ADS constructs preserved its ability to recognize its target, that the ADS was internalized by cells expressing the target, and that after cell internalization the drug was released and carried out its cytotoxic activity.

4. Conclusions

This study focused on designing and developing a more homogeneous ADC product in the effort to achieve a versatile and adaptable drug delivery system. A new drug delivery platform based on a non-covalent interaction between mAbs and an Fc-binding molecule (FcBM), which also acts as drug-carrier, was investigated here. As it is well known that SpA and SpG are able to bind the Fc region of many immunoglobulins with high affinity, they were chosen as the FcBM models. The proteins were successively PEGylated at the N-terminal

amino acid with a heterobifunctional PEG that was in turns conjugated to a drug or a dye. ITC and DLS analyses showed that the PEGylated FcBMs non-covalently bound mAbs with high affinity by simply mixing, thus creating the PEG-FcBM/mAbs complex. After the complexation with a model mAb (Trz or Rtx), Cy5 labeled ADSs were tested *in vitro* via cytometry analysis that showed high selectivity for the targeted antigen expressing cells. The preformed ADS proved to be stable even after incubation with a competitive antibody, maintaining the ability to recognize the target cells. From the study, SpG emerged as promising Fc-binding molecule for such application thanks to the feature of its PEGylated form to bind the target mAb with a binding ratio of 1:1, allowing a reduction of the heterogeneity of the system. Consequently, the toxin TubA was conjugated to PEG-SpG to get the TubA-PEG_{20kDa}-SpG/Trz ADS. As expected this ADS showed a preferential cytotoxic activity against the HER2/neu^+ cell line (SK-BR-3) with respect to the HER2/neu^- cell line (MDA-MB-231), thus supporting its application for both therapeutic purposes.

To conclude, an ADS approach was used to create a non-covalent drug delivery system utilizing an antibody as the targeting moiety that preserved an *in vitro* affinity for antigen presenting cells. Using this approach means that the number of drug molecules delivered by a single antibody can be strictly controlled, and as only the Fc region is involved in FcBM binding, this ensures that the Fab regions remain free to interact with the target antigen. As different antibodies can be used with the same FcBM construct, it is possible to select the most opportune mAb depending on cancer that is being treated.

Acknowledgement

The study was supported by "Fondazione AIRC per la Ricerca sul Cancro" (IG2017, Cod. 20224) and the University of Padova (STARS-WiC).

Appendix A. Supplementary material

Detailed characterization of SpA and SpG conjugates, TubA analysis and a calibration curve of reduced TubA in RP-HPLC. Expression of CD20 and HER2/neu in the several cell lines used. Supplementary data to this article can be found online at https://doi.org/10.1016/j.ejpb.2019.06.012.

References

[1] A.M. Wu, P.D. Senter, Arming antibodies: prospects and challenges for immunoconjugates, Nat. Biotechnol. 23 (2005) 1137–1146.
[2] E.L. Sievers, P.D. Senter, Antibody-drug conjugates in cancer therapy, Annu. Rev. Med. 64 (2013) 15–29.
[3] R. Bakhtiar, Antibody drug conjugates, Biotechnol. Lett. 38 (2016) 1655–1664.
[4] N. Diamantis, U. Banerji, Antibody-drug conjugates—an emerging class of cancer treatment, Br. J. Cancer. 114 (2016) 362–367.
[5] L. Ducry, B. Stump, Antibody-drug conjugates: linking cytotoxic payloads to monoclonal antibodies, Bioconj. Chem. 21 (2010) 5–13.
[6] R. Gébleux, G. Casi, Antibody-drug conjugates: current status and future perspectives, Pharmacol. Ther. 167 (2016) 48–59.
[7] H.L. Perez, P.M. Cardarelli, S. Deshpande, S. Gangwar, G.M. Schroeder, G.D. Vite, R.M. Borzilleri, Antibody-drug conjugates: current status and future directions, Drug Discov. Today 19 (2014) 869–881.
[8] M.E. Ackerman, D. Pawlowski, K.D. Wittrup, Effect of antigen turnover rate and expression level on antibody penetration into tumor spheroids, Mol. Cancer Ther. 7 (2008) 2233–2240.
[9] K.J. Hamblett, P.D. Senter, D.F. Chace, M.M. Sun, J. Lenox, C.G. Cerveny, K.M. Kissler, S.X. Bernhardt, A.K. Kopcha, R.F. Zabinski, D.L. Meyer, J.A. Francisco, Effects of drug loading on the antitumor activity of a monoclonal antibody drug conjugate, Clin. Cancer Res. 15 (2004) 7063–7070.
[10] C.F. McDonagh, E. Turcott, L. Westendorf, J.B. Webster, S.C. Alley, K. Kim, J. Andreyka, I. Stone, K.J. Hamblett, J.A. Francisco, P. Carter, Engineered antibody-drug conjugates with defined sites and stoichiometries of drug attachment, Protein Eng. Des. Sel. 19 (2006) 299–307.
[11] J.R. Junutula, H. Raab, S. Clark, S. Bhakta, D.D. Leipold, S. Weir, Y. Chen, M. Simpson, S.P. Tsai, M.S. Dennis, Y. Lu, Y.G. Meng, C. Ng, J. Yang, C.C. Lee, E. Duenas, J. Gorrell, V. Katta, A. Kim, K. McDorman, K. Flagella, R. Venook, S. Ross, S.D. Spencer, W. Lee Wong, H.B. Lowman, R. Vandlen, M.X. Sliwkowski, R.H. Scheller, P. Polakis, W. Mallet, Site-specific conjugation of a cytotoxic drug to an antibody improves the therapeutic index, Nat. Biotechnol. 26 (2008) 925–932.
[12] B.Q. Shen, K. Xu, L. Liu, H. Raab, S. Bhakta, M. Kenrick, K.L. Parsons-Reponte, J. Tien, S.-F. Yu, E. Mai, D. Li, J. Tibbitts, J. Baudys, O.M. Saad, S.J. Scales, P.J. McDonald, P.E. Hass, C. Eigenbrot, T. Nguyen, W.A. Solis, R.N. Fuji, K.M. Flagella, D. Patel, S.D. Spencer, L.A. Khawli, A. Ebens, W.L. Wong, R. Vandlen, S. Kaur, M.X. Sliwkowski, R.H. Scheller, P. Polakis, J.R. Junutula, Conjugation site modulates the in vivo stability and therapeutic activity of antibody-drug conjugates, Nat. Biotechnol. 30 (2012) 184–189.
[13] C.R. Behrens, B. Liu, Methods for site-specific drug conjugation to antibodies, MAbs 6 (2014) 46–53.
[14] S. Jeger, K. Zimmermann, A. Blanc, J. Grünberg, M. Honer, P. Hunziker, H. Struthers, R. Schibli, Site-specific and stoichiometric modification of antibodies by bacterial transglutaminase, Angew. Chem. – Int. Ed. 49 (2010) 9995–9997.
[15] E.S. Zimmerman, T.H. Heibeck, A. Gill, X. Li, C.J. Murray, M.R. Madlansacay, C. Tran, N.T. Uter, G. Yin, P.J. Rivers, A.Y. Yam, W.D. Wang, A.R. Steiner, S.U. Bajad, K. Penta, W. Yang, T.J. Hallam, C.D. Thanos, A.K. Sato, Production of site-specific antibody-drug conjugates using optimized non-natural amino acids in a cell-free expression system, Bioconjug. Chem. 25 (2014) 351–361.
[16] F. Tian, Y. Lu, A. Manibusan, A. Sellers, H. Tran, Y. Sun, T. Phuong, R. Barnett, B. Hehli, F. Song, M.J. DeGuzman, S. Ensari, J.K. Pinkstaff, L.M. Sullivan, S.L. Biroc, H. Cho, P.G. Schultz, J. DiJoseph, M. Dougher, D. Ma, R. Dushin, M. Leal, L. Tchistiakova, E. Feyfant, H.P. Gerber, P. Sapra, A general approach to site-specific antibody drug conjugates, Proc. Natl. Acad. Sci. U.S.A. 111 (2014) 1766–1771.
[17] E. Boeggeman, B. Ramakrishnan, M. Pasek, M. Manzoni, A. Puri, K.H. Loomis, T.J. Waybright, P.K. Qasba, Site specific conjugation of fluoroprobes to the remodeled Fc N-glycans of monoclonal antibodies using mutant glycosyltransferases: application for cell surface antigen detection, Bioconjug. Chem. 20 (2009) 1228–1236.
[18] L.N. Lund, T. Christensen, E. Toone, G. Houen, A. Staby, P.M. St, Hilaire, Exploring variation in binding of Protein A and Protein G to immunoglobulin type G by isothermal titration calorimetry, J. Mol. Recognit. 24 (2011) 945–952.
[19] P.K. Peterson, J. Verhoef, L.D. Sabath, P.G. Quie, Effect of protein A on staphylococcal opsonization, Infect. Immun. 15 (1977) 760–764.
[20] J.H. Dossett, G. Kronvall, R.C. Williams, P.G. Quie, Antiphagocytic effects of staphylococcal protein A, J. Immunol. 103 (1969) 1405–1410.
[21] K. Huse, H.J. Bohme, G.H. Scholz, Purification of antibodies by affinity chromatography, J. Biochem. Biophys. Methods. 51 (2002) 217–231.
[22] S. Hober, K. Nord, M. Linhult, Protein A chromatography for antibody purification, J. Chromatogr. B Anal. Technol. Biomed Life Sci. 848 (2007) 40–47.
[23] B. Akerstrom, L. Bjorck, A physicochemical study of protein G, a molecule with unique immunoglobulin G-binding properties, J. Biol. Chem. 261 (1986) 10240–10247.
[24] J.J. Langone, M.D. Boyle, T. Borsos, Studies on the interaction between protein A and immunoglobulin G. I. Effect of protein A on the functional activity of IgG, J. Immunol. 121 (1978) 327–332.
[25] A. Forsgren, J. Sjoquist, "Protein A" from S. aureus. I. Pseudo-immune reaction with human gamma-globulin, J. Immunol. 97 (1966) 822–827.
[26] A.E. Sauer-Eriksson, G.J. Kleywegt, M. Uhlén, T.A. Jones, Crystal structure of the C2 fragment of streptococcal protein G in complex with the Fc domain of human IgG, Structure 3 (1995) 265–278.
[27] T. Gallagher, P. Alexander, P. Bryan, G.L. Gilliland, Two crystal structures of the B1 immunoglobulin-binding domain of streptococcal protein G and comparison with NMR, Biochemistry 33 (1994) 4721–4729.
[28] A. Achari, S.P. Hale, A.J. Howard, G.M. Clore, A.M. Gronenborn, K.D. Hardman, M. Whitlow, 1.67-A X-ray structure of the B2 immunoglobulin-binding domain of streptococcal protein G and comparison to the NMR structure of the B1 domain, Biochemistry 31 (1992) 10449–10457.
[29] J. Deisenhofer, Crystallographic refinement and atomic models of a human Fc fragment and its complex with fragment B of protein A from Staphylococcus aureus at 2.9- and 2.8-A resolution, Biochemistry 20 (1981) 2361–2370.
[30] A.M. Gronenborn, G.M. Clore, Identification of the contact surface of a streptococcal protein G domain complexed with a human Fc Fragment, J. Mol. Biol. 233 (1993) 331–335.
[31] L.Y. Lian, J.C. Yang, J.P. Derrick, M.J. Sutcliffe, G.C. Roberts, J.P. Murphy, C.R. Goward, T. Atkinson, Sequential 1H NMR assignments and secondary structure of an IgG-binding domain from protein G, Biochemistry 30 (1991) 5335–5340.
[32] A.M. Gronenborn, D.R. Filpula, N.Z. Essig, A. Achari, M. Whitlow, P.T. Wingfield, G.M. Clore, A novel, highly stable fold of the immunoglobulin binding domain of streptococcal protein G, Science 253 (1991) 657–661.
[33] H. Gouda, H. Torigoe, A. Saito, M. Sato, Y. Arata, I. Shimada, Three-dimensional solution structure of the B domain of staphylococcal protein A: comparisons of the solution and crystal structures, Biochemistry 31 (1992) 9665–9672.
[34] A. Arouri, P. Garidel, W. Kliche, A. Blume, Hydrophobic interactions are the driving force for the binding of peptide mimotopes and Staphylococcal protein A to recombinant human IgG1, Eur. Biophys. J. 36 (2007) 647–660.
[35] T. Moks, L. Abrahmsén, B. Nilsson, U. Hellman, J. Sjoquist, M. Uhlén, Staphylococcal protein A consists of five IgG-binding domains, Eur. J. Biochem. 156 (1986) 637–643.
[36] I. Bjork, B.A. Petersson, J. Sjoquist, Some physicochemical properties of protein A from staphylococcus aureus, Eur. J. Biochem. 29 (1972) 579–584.
[37] J. Sjöquist, Protein A from Staphylococcus aureus, FEBS Lett. 28 (1972) 73–76.
[38] U. Sjöbring, L. Björck, W. Kastern, Streptococcal Protein G. Gene structure and protein binding properties, J. Biol. Chem. 266 (1991) 399–405.
[39] A. Olsson, M. Eliasson, B. Guss, B. Nilsson, U. Hellman, M. Lindberg, M. Uhlén, Structure and evolution of the repetitive gene encoding streptococcal protein G,

Eur. J. Biochem. 168 (1987) 319–324.
[40] S.R. Fahnestock, P. Alexander, J. Nagle, D. Filpula, Gene for an immunoglobulin-binding protein from a group G streptococcus, J. Bacteriol. 167 (1986) 870–880.
[41] B. Guss, M. Eliasson, A. Olsson, M. Uhlén, A.K. Frej, H. Jörnvall, J.I. Flock, M. Lindberg, Structure of the IgG-binding regions of streptococcal protein G, EMBO J. 5 (1986) 1567–1575.
[42] B. Akerström, E. Nielsen, L. Björck, Definition of IgG- and albumin-binding regions of streptococcal protein G, J. Biol. Chem. 262 (1987) 13388–13391.
[43] M. Linhult, H.K. Binz, M. Uhlén, S. Hober, Mutational analysis of the interaction between albumin-binding domain from streptococcal protein G and human serum albumin, Protein Sci. 11 (2002) 206–213.
[44] B. Jansson, M. Uhlén, P.Å. Nygren, All individual domains of staphylococcal protein A show Fab binding, FEMS Immunol. Med. Microbiol. 20 (1998) 69–78.
[45] P.W. Roben, A.N. Salem, G.J. Silverman, VH3 family antibodies bind domain D of staphylococcal protein A, J. Immunol. 154 (1995) 6437–6445.
[46] M. Graille, E.A. Stura, A.L. Corper, B.J. Sutton, M.J. Taussig, J.B. Charbonnier, G.J. Silverman, Crystal structure of a Staphylococcus aureus protein A domain complexed with the Fab fragment of a human IgM antibody: structural basis for recognition of B-cell receptors and superantigen activity, Proc. Natl. Acad. Sci. USA 97 (2000) 5399–5404.
[47] M.A. Starovasnik, M.P. O'Connell, W.J. Fairbrother, R.F. Kelley, Antibody variable region binding by Staphylococcal protein A: thermodynamic analysis and location of the Fv binding site on E-domain, Protein Sci. 8 (1999) 1423–1431.
[48] J.P. Derrick, D.B. Wigley, Crystal structure of a streptococcal protein G domain bound to an Fab fragment, Nature 359 (1992) 752–754.
[49] J. Baselga, L. Norton, J. Albanell, Y.M. Kim, J. Mendelsohn, Recombinant humanized anti-HER2 antibody (herceptin) enhances the antitumor activity of paclitaxel and doxorubicin against HER2/neu overexpressing human breast cancer xenografts, Cancer Res. 58 (1998) 2825–2831.
[50] M.M. Goldenberg, Trastuzumab, a recombinant DNA-derived humanized monoclonal antibody, a novel agent for the treatment of metastatic breast cancer, Clin. Ther. 21 (1999) 309–318.
[51] D.G. Maloney, A.J. Grillo-López, C.A. White, D. Bodkin, R.J. Schilder, J.A. Neidhart, N. Janakiraman, K.A. Foon, T. Liles, B.K. Dallaire, K. Wey, T. Davis, R. Levy, IDEC-C2B8 (Rituximab) anti-CD20 monoclonal antibody therapy in patients with relapsed low-grade non-Hodgkin's lymphoma, Blood 8 (2013) 2188–2195.
[52] D.R. Anderson, A. Grillo-López, C. Varns, K.S. Chambers, N. Hanna, Targeted anticancer therapy using rituximab, a chimaeric anti-CD20 antibody (IDEC-C2B8) in the treatment of non-Hodgkin's B-cell lymphoma, Biochem. Soc. Trans. 25 (1997) 705–708.
[53] P.K. Smith, R.I. Krohn, G.T. Hermanson, A.K. Mallia, F.H. Gartner, M.D. Provenzano, E.K. Fujimoto, N.M. Goeke, B.J. Olson, D.C. Klenk, Measurement of protein using bicinchoninic acid, Anal. Biochem. 150 (1985) 76–85.
[54] U.K. Laemmli, Cleavage of structural proteins during assembly of the head of bacteriophage T4, Nature 227 (1970) 680–685.
[55] M. Floreani, D. Gabbia, M. Barbierato, S. De Martin, P. Palatini, Differential inducing effect of benzo[a]pyrene on gene expression and enzyme activity of cytochromes P450 1A1 and 1A2 in Sprague-Dawley and Wistar rats, Drug Metab. Pharmacokinet. 27 (2012) 640–652.
[56] S.L. Snyder, P.Z. Sobocinski, An improved 2,4,6-trinitrobenzenesulfonic acid method for the determination of amines, Anal. Biochem. 64 (1975) 284–288.
[57] J. Carlsson, H. Drevin, R. Axén, Protein thiolation and reversible protein-protein conjugation. N-Succinimidyl 3-(2-pyridyldithio)propionate, a new heterobifunctional reagent, Biochem. J. 173 (1978) 723–737.
[58] P.K. Ngai, F. Ackermann, H. Wendt, R. Savoca, H.R. Bosshard, Protein A antibody-capture ELISA (PACE): an ELISA format to avoid denaturation of surface-adsorbed antigens, J. Immunol. Methods. 158 (1993) 267–276.
[59] M.N. Widjojoatmodjo, A.C. Fluit, R. Torensma, J. Verhoef, Comparison of immunomagnetic beads coated with protein A, protein G, or goat anti-mouse immunoglobulins. Applications in enzyme immunoassays and immunomagnetic separations, J. Immunol. Methods. 165 (1993) 11–19.
[60] Z. Wang, G. Jin, Feasibility of protein A for the oriented immobilization of immunoglobulin on silicon surface for a biosensor with imaging ellipsometry, J. Biochem. Biophys. Methods. 57 (2003) 203–211.
[61] Y. Meng, B. Chen, Protein A for human IgG oriented immobilization on silicon surface for an imaging ellipsometry biosensor, in: Proc. 31st Annu. Int. Conf. IEEE Eng. Med. Biol. Soc. Eng. Futur. Biomed. EMBC, 2009.
[62] I.M. Montagner, A. Merlo, D. Carpanese, A. Dalla Pietà, A. Mero, A. Grigoletto, A. Loregian, D. Renier, M. Campisi, P. Zanovello, G. Pasut, A. Rosato, A site-selective hyaluronan-interferonα2a conjugate for the treatment of ovarian cancer, J. Control. Release. 236 (2016) 79–89.
[63] A. Grigoletto, A. Mero, I. Zanusso, O. Schiavon, G. Pasut, Chemical and enzymatic site specific PEGylation of hGH: the stability and in vivo activity of PEG-N-Terminal-hGH and PEG-Gln141-hGH conjugates, Macromol. Biosci. 16 (2016) 50–56.
[64] C.R. Goward, J.P. Murphy, T. Atkinson, D.A. Barstow, Expression and purification of a truncated recombinant streptococcal protein G, Biochem. J. 267 (1990) 171–177.
[65] P. Nygren, M. Eliasson, L. Abrahmsén, M. Uhlén, E. Palmcrantz, Analysis and use of the serum albumin binding domains of streptococcal protein G, J. Mol. Recognit. 1 (1988) 69–74.
[66] C.S. Fishburn, The pharmacology of PEGylation: balancing PD with PK to generate novel therapeutics, J. Pharm. Sci. 97 (2008) 4167–4183.
[67] D. Dalzoppo, V. Di Paolo, L. Calderan, G. Pasut, A. Rosato, A.M. Caccuri, L. Quintieri, Thiol-activated anticancer agents: the state of the art, Anticancer. Agents Med. Chem. 17 (2017) 4–20.
[68] G. Saito, J.A. Swanson, K.D. Lee, Drug delivery strategy utilizing conjugation via reversible disulfide linkages: role and site of cellular reducing activities, Adv. Drug Deliv. Rev. 55 (2003) 199–215.